

Unified Chew-Mandelstam SAID analysis of pion photoproduction data

Ron L. Workman,¹ Mark W. Paris,^{1,*} William J. Briscoe,¹ and Igor I. Strakovsky¹

¹*Data Analysis Center at the Institute for Nuclear Studies,
Department of Physics
The George Washington University, Washington, D.C. 20052*
(Dated: November 15, 2018)

A unified description of single-pion photoproduction data, together with pion- and eta-hadron production data, has been achieved in a Chew-Mandelstam parametrization which is consistent with unitarity at the two-body level. Energy-dependent and single-energy partial wave analyses of pion photoproduction data have been performed and compared to previous SAID fits and multipoles from the Mainz and Bonn-Gatchina groups.

PACS numbers: 13.75.Gx, 13.60.-r, 11.55.Bq, 11.80.Et, 11.80.Gw, 13.60.Le

I. INTRODUCTION

A wealth of $\gamma N \rightarrow \pi N$ data, for single- and double-polarization observables, is anticipated from electromagnetic facilities worldwide over the coming months and years. These data will be pivotal in determining the underlying amplitudes in complete experiments, and in discerning between various microscopic models of multi-channel reaction theory.

The focus of precision electromagnetic measurements, over the nucleon resonance region, is to more fully map the non-perturbative regime of quantum chromodynamics, the fundamental theory of the strong interaction, to shed light on its confining and chiral symmetry breaking properties. These electromagnetic data take the field to the next and necessary level of precision. This is required in order to obtain a theoretical description of the nucleon that both explains and subsumes the simple constituent quark model, which has provided a qualitative picture of nucleon structure and reactions. The expected data heralds an era of precision hadron spectroscopy, particularly for baryons, and has ushered in a renaissance in hadronic reaction theory. Significant refinements in the quality and quantity of available data offer the opportunity to develop more sophisticated models of hadronic reactions, constrained by fundamental principles of field theory, such as unitarity and gauge invariance, which have model dependencies under better control, if not eliminated. Such a complete and successful phenomenology would appear to be a prerequisite for a deeper understanding in terms of quarks and gluons [1].

The present manuscript details multipole analyses of the single-pion photoproduction data using a parametrization form related to, but an improvement upon, previous SAID parametrizations [2–4]. The energy-dependent (ED) analysis is performed over the center-of-mass energy (W) range from the near-threshold region to about 2.5 GeV, including resonances through

the fourth resonance region. We also generate single energy solutions (SES), which fit the data over narrow energy bins assuming phase information obtained from the ED solutions. The relations between ED and SES fits have been extensively studied in Ref. [5]. A detailed discussion of amplitude and observable conventions is also given in this source.

The fitted pion-photoproduction database is identical to that used in our most recent [4] SN11 analysis, based on the standard SAID parametrization. In the following section, we compare the previous and present SAID fit forms used to analyze these data. Extracted multipoles are compared to previous SAID fits, and those from other groups, in Sec. III. Our results and their implications are summarized in Sec. IV.

II. FORMALISM

The Chew-Mandelstam (CM) energy-dependent (ED) parametrization for the hadronic T matrix, described in Ref. [6], has been used in a recent coupled-channel fit of πN elastic scattering and $\pi N \rightarrow \eta N$ reaction data. It gives a realistic description of the data with χ^2 per datum better than any other parametrization or model, to our knowledge [7, 8]. The parametrization form used in this fit is given as

$$T_{\alpha\beta} = \sum_{\sigma} [1 - \overline{K}C]_{\alpha\sigma}^{-1} \overline{K}_{\sigma\beta}, \quad (1)$$

where α , β , and σ are indices for the considered channels, πN , $\pi\Delta$, ρN , and ηN . This parametrization has been discussed in Refs. [6, 9, 10]. Given the success of this approach in the hadronic two-body sector, its application to the study of meson photoproduction is warranted. The main result of the present study is the use of the information encoded in Eq. (1) by employing the factor $[1 - \overline{K}(W)C(W)]^{-1}$ (called the “hadronic rescattering matrix”) in the photoproduction parametrization form.

The CM form of Eq. (1) may be extended to include

* Present address: Theoretical Division, Los Alamos National Laboratory, Los Alamos, NM 87545, USA

the electromagnetic channel as:

$$T_{\alpha\gamma} = \sum_{\sigma} [1 - \overline{KC}]_{\alpha\sigma}^{-1} \overline{K}_{\sigma\gamma}. \quad (2)$$

Here, γ denotes the electromagnetic channel, γN , and σ denotes the hadronic channels which appear in the parametrization of the hadronic rescattering matrix, $[1 - \overline{KC}]^{-1}$. Note that by sharing the common factor, $[1 - \overline{KC}]^{-1}$ which encodes, at least qualitatively speaking, the hadronic channel coupling (or rescattering) effects, Eqs. (1) and (2) constitute a unified approach to the problem of parametrizing the hadronic scattering and photoproduction amplitudes.

We pause here to make several remarks about the analytic form of the parametrization and its use in the present study. We first note that since the CM K-matrix $\overline{K}_{\sigma\gamma}(W)$ is a polynomial in the center-of-mass energy, W , an entire function, non-analytic points in the complex- W plane are all a result of the hadronic rescattering matrix, $[1 - \overline{KC}]^{-1}$. This matrix has branch points and poles consistent with two-body and quasi-two-body unitarity [11]. The quasi-two-body channels, $\pi\Delta$ and ρN model the three-body $\pi\pi N$ channel only approximately. We use Eqs. (1) and (2) as follows. The parameters of the hadronic CM K-matrix, $\overline{K}_{\alpha,\beta}$, where α and β may include (depending on the partial wave) πN , $\pi\Delta$, ρN , and ηN are fixed by fitting the $\pi N \rightarrow \pi N$ and $\pi N \rightarrow \eta N$ data as in Ref. [6]. The π -photoproduction data is then fitted [12] by varying only the parameters of the electromagnetic CM K-matrix elements, $\overline{K}_{\sigma\gamma}$, where σ includes the channels πN , $\pi\Delta$, ρN , and ηN .

This approach differs markedly from that adopted in Refs. [3, 4, 13, 14]. There, the fit form, motivated by a multichannel Heitler K-matrix approach [15],

$$M = (\text{Born} + A)(1 + iT_{\pi N}) + BT_{\pi N}, \quad (3)$$

was modified to include a term

$$(C + iD)(\text{Im}T_{\pi N} - |T_{\pi N}|^2), \quad (4)$$

where $T_{\pi N}$ is the elastic πN scattering partial-wave amplitude associated with the pion-photoproduction multipole amplitude M . The added piece, which grows with the πN reaction cross section, was found to improve the fit at energies above the ηN threshold. Each of the phenomenological terms A to D was parameterized as a polynomial in energy, having the correct threshold behavior.

In the new form, terms A and B have been effectively replaced by a single CM K-matrix element, $\overline{K}_{\pi\gamma}$. Conversely, the influence of channels opening above πN is now (more correctly) associated with individual channels (ηN , $\pi\Delta$, and ρN) rather than a single term. Large cancellations found to occur between the Born, A , and B terms suggested that a more economical parametrization is possible [15]. In fact, the CM K-matrix form provides a better overall fit to the data with fewer free parameters, as we will show in the next section.

III. FIT RESULTS AND MULTIPOLE AMPLITUDES

In Table I, the fit quality and number of searched parameters is compared for the two fit forms discussed in the previous section. Here we have used the same database to 2.7 GeV as was used in generating solution SN11 [4]. The present CM12 form requires fewer parameters to achieve a slightly better data fit. The energy-dependence of this result was tested by repeating the analyses over three different energy ranges.

As the fit employs polynomial functions for A to D , of SN11, or the electromagnetic CM K-matrix elements of CM12, a subjective criteria is required to determine the order of polynomials fitted. In the fits to 2.7 GeV, the order of polynomial functions was increased until further additions improved the overall χ^2 by 50 or less. This same criteria was used in both the SN11 and CM12 fits, in order to have a basis for comparison. As more parameters were searched, their ability to improve the fit diminished. In the fits to lower energy limits, parameters were removed in steps, again with the condition that removing a parameter should not increase the overall χ^2 by more than 50.

In Figures 1–6, we compare SN11 and CM12 to MAID07 [16] and Bonn-Gatchina [17] fits. Only proton-target multipoles are presented, as changes in the neutron-target database are likely to alter these fits in the near future. For resonances with a canonical Breit-Wigner shape, such as the $\Delta(1232)P_{33}$, $N(1520)D_{13}$, $N(1680)F_{15}$, and $\Delta(1950)F_{37}$, all solutions agree fairly well in the neighborhood of the resonance energy. The fit CM12 deviates significantly from SN11 in the $E_{0+}^{1/2}$ multipole. The CM12 phase behavior, from threshold up to the peak of the $N(1535)S_{11}$ resonance, differs from SN11 and MAID07, but is qualitatively similar to the Bonn-Gatchina result, as shown in Figure 7. While both SN11 and MAID07 essentially follow the S_{11} pion-nucleon phase up to the ηN threshold cusp, the CM12 and Bonn-Gatchina fits depart from this phase above the two-pion production threshold.

Some structures occurring in SN11, between threshold and the first resonance energies, are missing or diminished in CM12. Examples are the real parts of $M_{1-}^{3/2}$, $M_{1+}^{1/2}$, and $E_{3-}^{1/2}$. In each of these cases, the CM12 fit more closely resembles the MAID07 and Bonn-Gatchina results. This reflects the fact that the replacement of the phenomenological terms A and B of Eq. (3) with a single CM K-matrix element in Eq. (2) is more form-restrictive.

In Fig. 8, we compare the χ^2/data of the ED and SES fits over energy bins used to generate the SES. As in Ref. [4], we see a noticeable increase in the χ^2 difference above about 800 MeV. In Fig. 9, we compare χ^2 values for SES generated from the SN11 and CM12 fits over identical energy bins. As multipole phases are fixed for multipoles searched in generating these SES [5], this serves as a comparison of the, often quite different, phases

found in SN11 and CM12. While the SN11 SES achieve a better fit in the near-threshold region, between 700 and 1100 MeV the CM12 SES consistently give the better fit.

TABLE I. χ^2/data and number of searched parameters (N_p) compared for fits to pion photoproduction data over varied energy ranges. The fit form used for solution SN11 [4] is compared to the Chew-Mandelstam form, CM12. See text for details.

Solution	Energy limit (MeV)	χ^2/N_{Data}	N_p
SN11	2700	2.08	209
CM12	2700	2.01	200
SN11a	2100	1.96	206
CM12a	2100	1.88	194
SN11b	1200	1.69	175
CM12b	1200	1.64	166

IV. SUMMARY AND CONCLUSION

We have fitted the single-pion photoproduction database utilizing a parametrization consistent with the Chew-Mandelstam form used in our previous fits to πN scattering and ηN production data. This new fit has a number of interesting features. It is more economical, using fewer parameters to obtain a slightly better overall fit. Some low-energy structures, not seen by other groups, have disappeared in the present fit. The phase behavior of the $E_{0+}^{1/2}$ has changed significantly and now is qualitatively similar to the Bonn-Gatchina result.

Comparison of the ED and SES fits shows, as was found in Ref. [4], a rise in χ^2 difference, evaluated over narrow energy bins, above about 800 MeV in the photon energy. This could be related to the energy limit of MAMI-B, which has contributed a significant fraction of the precise data below 800 MeV (thus, a data issue) or due to the treatment of channels above single-pion production (a model issue). The comparison of SES fits, derived from the ED SN11 and CM12 solutions, suggests that the CM12 multipole phases, held fixed in SES, are preferred in the intermediate-energy region.

In Table II, we compare photo-decay couplings extracted from CM12 and SN11, using the method of Ref. [4], to the average of PDG values. As expected, the $N(1535)S_{11}$ shows a large increase to 128 ± 4 (in $(\text{GeV})^{-1/2} \times 10^{-3}$ units), compared to 105 ± 10 from the Bonn-Gatchina group, and 118 found in Eta-MAID [20]. As in the SN11 analysis, the $N(1650)S_{11}$ is very difficult to fit using this procedure. The fit prefers a larger Breit-Wigner mass and width, and a lower value for Γ_π/Γ . Allowing for these variations, as reflected in its uncertainty, the value quoted here should be taken only as a rough estimate.

Other couplings are generally either close to values

TABLE II. Resonance parameters for N^* and Δ^* states from the SAID fit to the πN data [6] (second column) and proton helicity amplitudes $A_{1/2}$ and $A_{3/2}$ (in $[(\text{GeV})^{-1/2} \times 10^{-3}]$ units) from the CM12 solution (first row), the SN11 [4] solution (second row), and average values from the PDG10 [18] (third row).

Resonance	πN SAID	$A_{1/2}$	$A_{3/2}$
$N(1535)S_{11}$	$W_R=1547$ MeV	128 ± 4	
	$\Gamma=188$ MeV	99 ± 2	
	$\Gamma_\pi/\Gamma=0.36$	90 ± 30	
$N(1650)S_{11}$	$W_R=1635$ MeV	55 ± 30	
	$\Gamma=115$ MeV	65 ± 25	
	$\Gamma_\pi/\Gamma=1.00$	53 ± 16	
$N(1440)P_{11}$	$W_R=1485$ MeV	-56 ± 1	
	$\Gamma=284$ MeV	-58 ± 1	
	$\Gamma_\pi/\Gamma=0.79$	-65 ± 4	
$N(1720)P_{13}$	$W_R=1764$ MeV	95 ± 2	-48 ± 2
	$\Gamma=210$ MeV	99 ± 3	-43 ± 2
	$\Gamma_\pi/\Gamma=0.09$	18 ± 30	-19 ± 20
$N(1520)D_{13}$	$W_R=1515$ MeV	-19 ± 2	141 ± 2
	$\Gamma=104$ MeV	-16 ± 2	156 ± 2
	$\Gamma_\pi/\Gamma=0.63$	-24 ± 9	166 ± 5
$N(1675)D_{15}$	$W_R=1674$ MeV	13 ± 1	16 ± 1
	$\Gamma=147$ MeV	13 ± 2	19 ± 2
	$\Gamma_\pi/\Gamma=0.39$	19 ± 8	15 ± 9
$N(1680)F_{15}$	$W_R=1680$ MeV	-7 ± 2	140 ± 2
	$\Gamma=128$ MeV	-13 ± 3	141 ± 3
	$\Gamma_\pi/\Gamma=0.70$	-15 ± 6	133 ± 12
$\Delta(1620)S_{31}$	$W_R=1615$ MeV	29 ± 3	
	$\Gamma=147$ MeV	64 ± 2	
	$\Gamma_\pi/\Gamma=0.32$	27 ± 11	
$\Delta(1232)P_{33}$	$W_R=1233$ MeV	-139 ± 2	-262 ± 3
	$\Gamma=119$ MeV	-138 ± 3	-259 ± 5
	$\Gamma_\pi/\Gamma=1.00$	-135 ± 6	-250 ± 8
$\Delta(1700)D_{33}$	$W_R=1695$ MeV	105 ± 5	92 ± 4
	$\Gamma=376$ MeV	109 ± 4	84 ± 2
	$\Gamma_\pi/\Gamma=0.16$	104 ± 15	85 ± 22
$\Delta(1905)F_{35}$	$W_R=1858$ MeV	19 ± 2	-38 ± 4
	$\Gamma=321$ MeV	9 ± 3	-46 ± 3
	$\Gamma_\pi/\Gamma=0.12$	26 ± 11	-45 ± 20
$\Delta(1950)F_{37}$	$W_R=1921$ MeV	-83 ± 4	-96 ± 4
	$\Gamma=271$ MeV	-71 ± 2	-92 ± 2
	$\Gamma_\pi/\Gamma=0.47$	-76 ± 12	-97 ± 10

found in SN11, or are within the PDG ranges. The $N(1520)D_{13}$ $A_{3/2}$ (141 ± 2) has dropped below the PDG range (166 ± 5), but is above the Bonn-Gatchina value of 131 ± 10 . The $N(1720)P_{13}$ couplings remain very uncertain, as is clear from the multipole plot comparison. Here the present PDG range is certainly too narrow - the Bonn-Gatchina result for $A_{3/2}$ is 150 ± 30 , compared

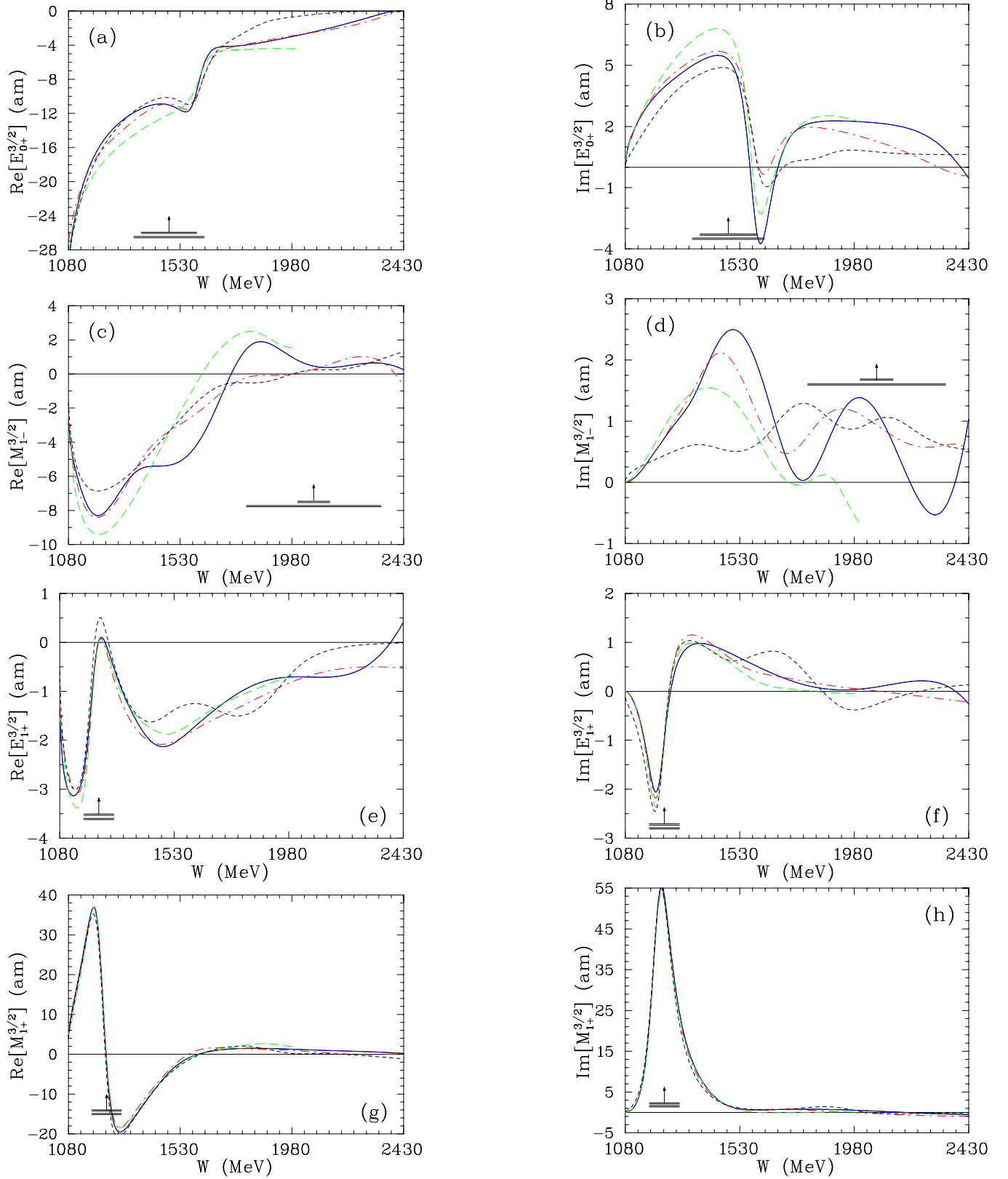


FIG. 1. (Color online) $I=3/2$ multipole amplitudes from threshold to $W = 2.43$ GeV ($E_\gamma = 2.7$ GeV). Solid (dash-dotted) lines correspond to the SN11 (CM12) solution. Short-dashed (dashed) lines give BG2010-02 solution [17] (MAID07 [16], which terminates at $W=2$ GeV). Vertical arrows indicate resonance energies, W_R , and horizontal bars show full (Γ) and partial ($\Gamma_{\pi N}$) widths associated with the SAID πN solution SP06 [6].

to the PDG range -19 ± 20 . For $A_{1/2}$, the PDG range is 18 ± 30 , with the CM12, SN11, and Bonn-Gatchina results all near 100.

ACKNOWLEDGMENTS

This work was supported in part by the U.S. Department of Energy Grant DE-FG02-99ER41110.

-
- [1] M. R. Pennington, arXiv: 1109.3690 [nucl-th].
- [2] R. A. Arndt, R. L. Workman, Zhujun Li, and L. D. Roper, Phys. Rev. C **42** 1853 (1990).
- [3] R.A. Arndt, W.J. Briscoe, I.I. Strakovsky, and R.L. Workman, Phys. Rev. C **66**, 055213 (2002).
- [4] R. L. Workman, W. J. Briscoe, M. W. Paris, and I. I. Strakovsky, to be published in Phys. Rev. C (2012); arXiv: 1109.0722 [hep-ph].
- [5] R. L. Workman *et al.*, Eur. Phys. J. A **47**, 143 (2011).
- [6] R. A. Arndt, W. J. Briscoe, I. I. Strakovsky, and R. L. Workman, Phys. Rev. C **74**, 045205 (2006).
- [7] R.A. Arndt, W.J. Briscoe, M.W. Paris, I.I. Strakovsky, and R.L. Workman, Chinese Phys. C **33**, 1063 (2009).
- [8] M. W. Paris and R. L. Workman, Phys. Rev. C **82**, 035202 (2010).
- [9] R. A. Arndt, J. M. Ford, and L. D. Roper, Phys. Rev. D **32**, 1085 (1985).
- [10] R. A. Arndt, I. I. Strakovsky, R. L. Workman, and M. M. Pavan, Phys. Rev. C **52**, 2120 (1995).
- [11] R. J. Eden P. V. Landshoff, D. I. Olive, and J. C. Polkinghorne, *The Analytic S-matrix*, (Cambridge University Press, Cambridge, 1966), pp. 231–232.
- [12] For multipoles with $\ell \geq 4$, the new form offers no advantage and unitarized Born terms were generally used. The $\Delta(1232)$, associated with a πN amplitude which remains elastic to much higher energies, is unaltered in the new fit.
- [13] M. Dugger *et al.* (CLAS Collaboration), Phys. Rev. C **76**, 025211 (2007).
- [14] M. Dugger *et al.* (CLAS Collaboration), Phys. Rev. C **79**, 065206 (2009).
- [15] R. L. Workman, Phys. Rev. C **74**, 055207 (2006).
- [16] The MAID analyses are available through the Mainz website: <http://wwwkph.kph.uni-mainz.de/MAID/>. See also D. Drechsel, S. S. Kamalov, and L. Tiator, Eur. Phys. J. A **34**, 69 (2007).
- [17] The Bonn-Gatchina analyses are available through the Bonn website: <http://pwa.hiskp.uni-bonn.de/>. See also A. V. Anisovich *et al.*, Eur. Phys. J A **44**, 203 (2010).
- [18] K. Nakamura, *et al.* (Particle Data Group), J. Phys. G **37**, 075201 (2010).
- [19] The SAID website contains data and fits for this and a number of other medium-energy reactions: <http://gwdac.phys.gwu.edu>.
- [20] W.-T. Chiang, *et al.*, Nucl. Phys. A **700**, 429 (2002).

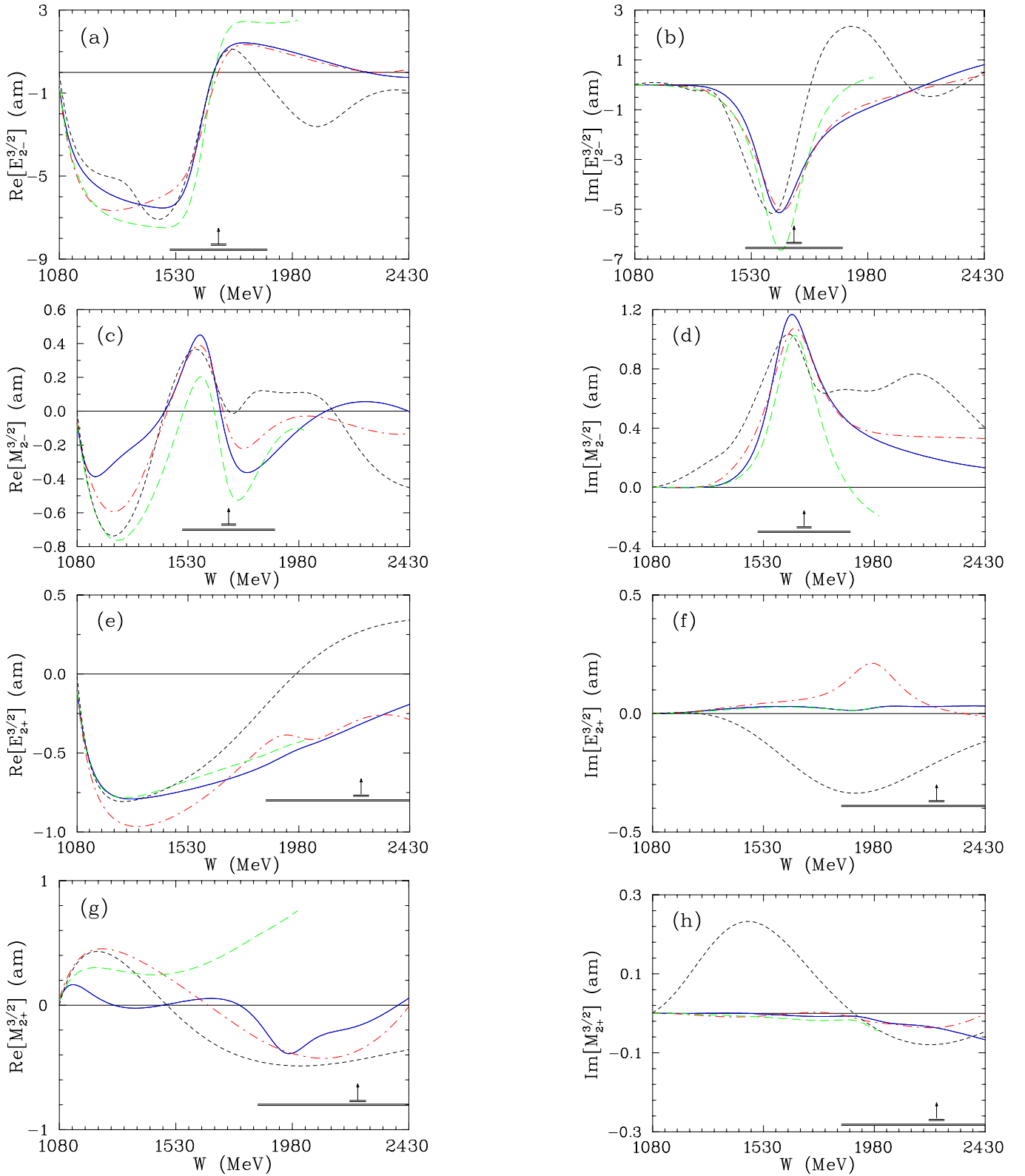


FIG. 2. (Color online) Notation of the multipoles is the same as in Fig. 1.

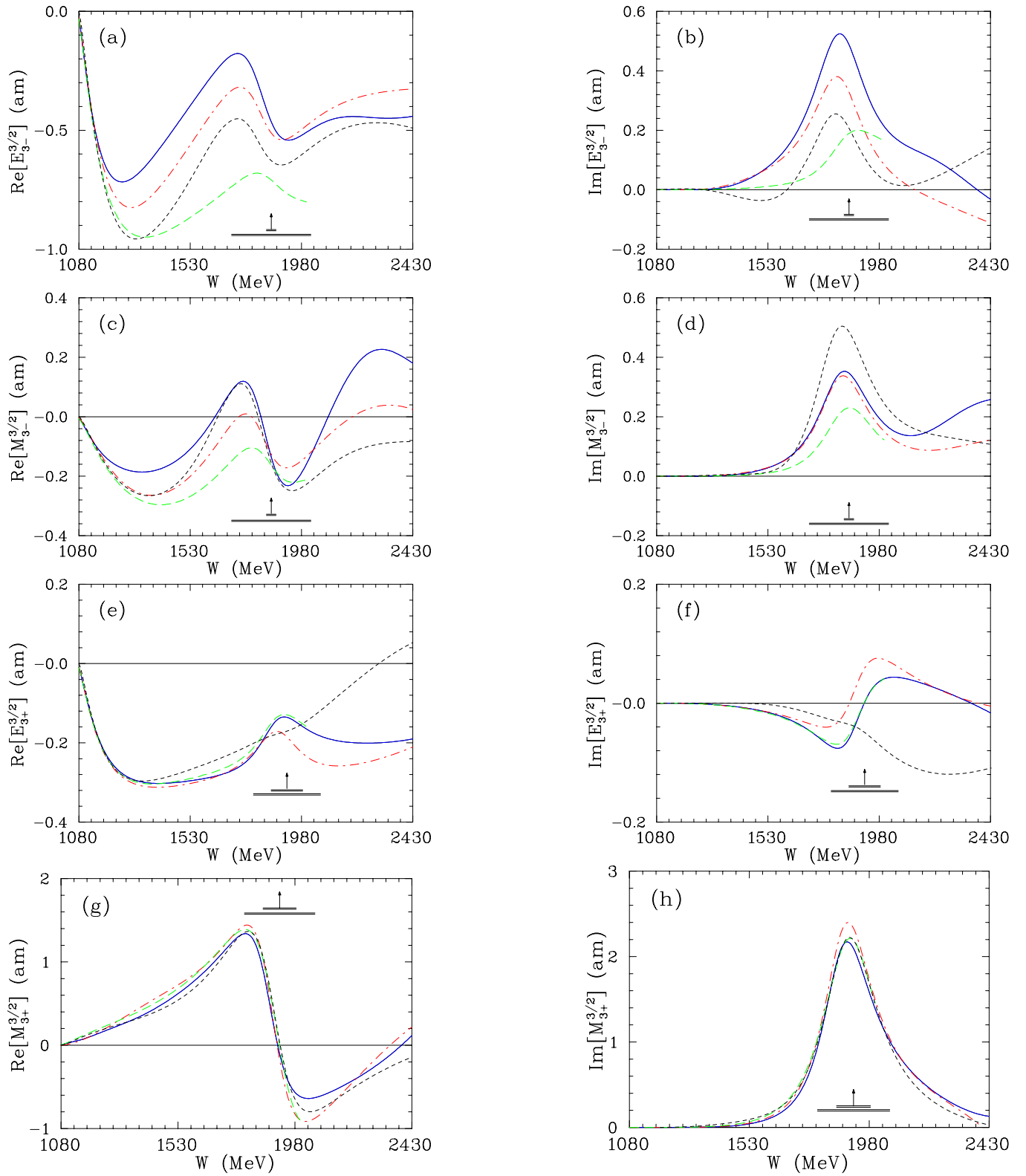


FIG. 3. (Color online) Notation of the multipoles is the same as in Fig. 1.

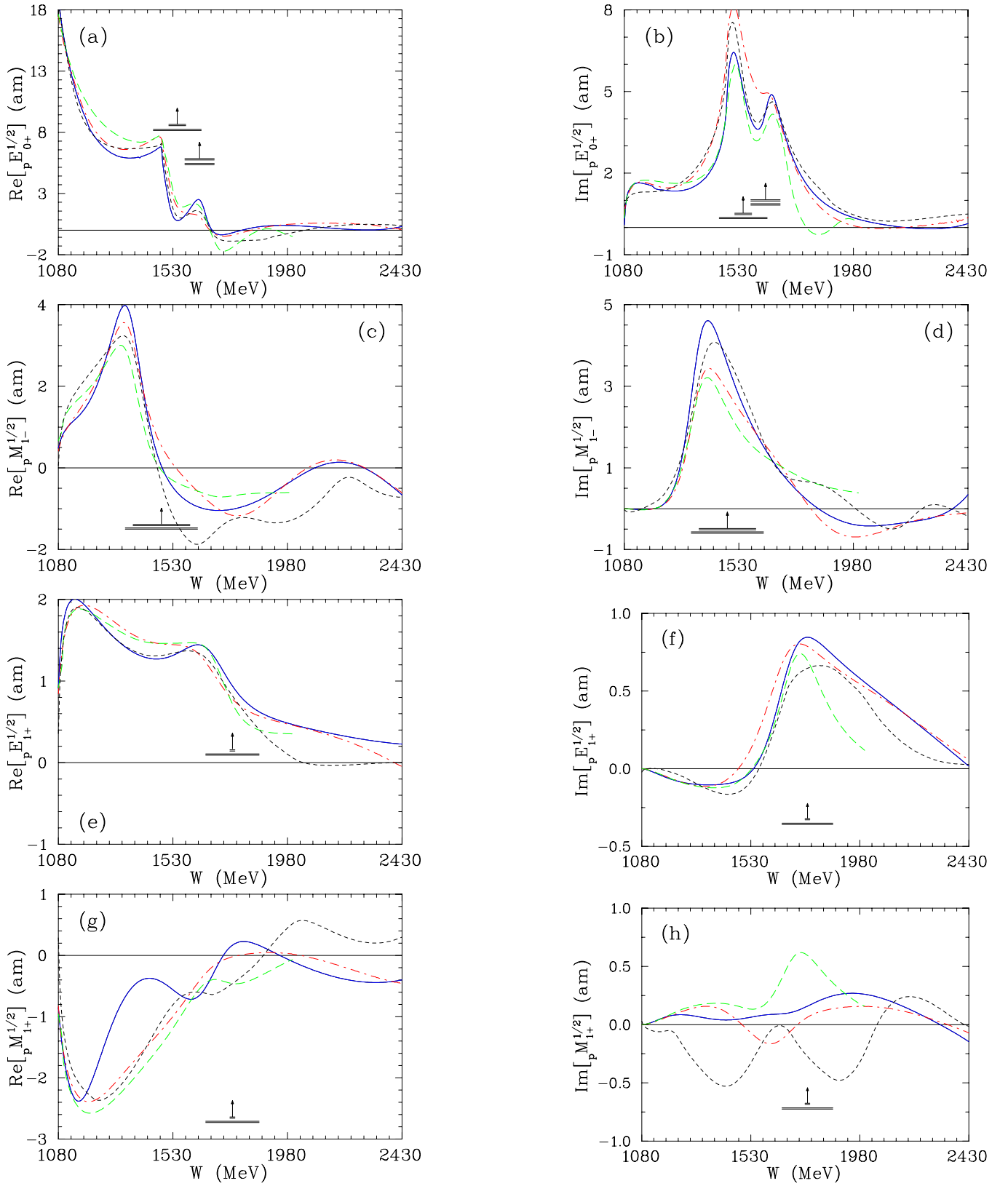


FIG. 4. (Color online) Proton multipole $I=1/2$ amplitudes from threshold to $W = 2.43$ GeV ($E_\gamma = 2.7$ GeV). Notation of the solutions is the same as in Fig. 1. Vertical arrows indicate resonance energies, W_R , and horizontal bars show full (Γ) and partial ($\Gamma_{\pi N}$) widths associated with the SAID πN solution SP06 [6].

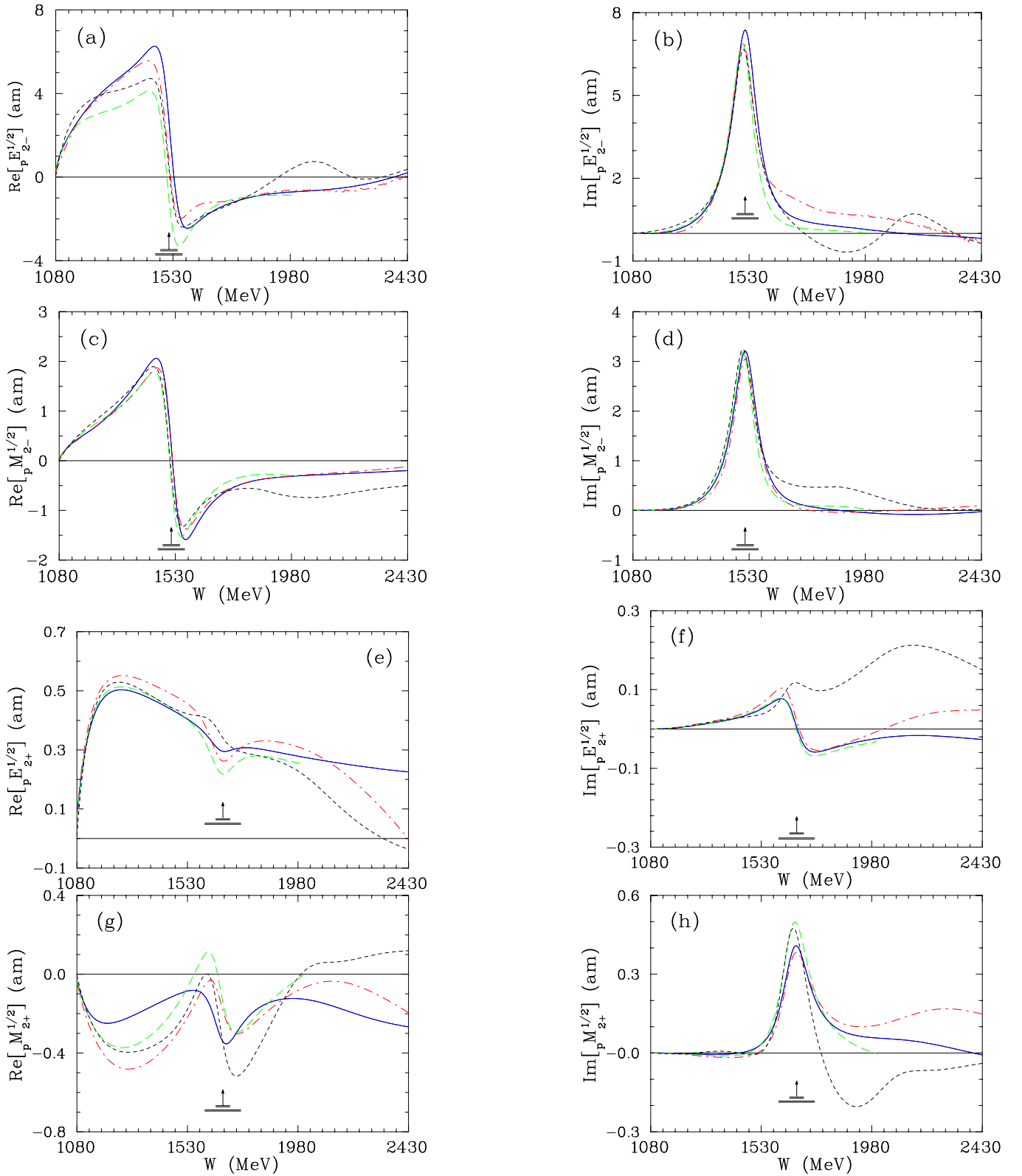


FIG. 5. (Color online) Notation of the multipoles is the same as in Fig. 4.

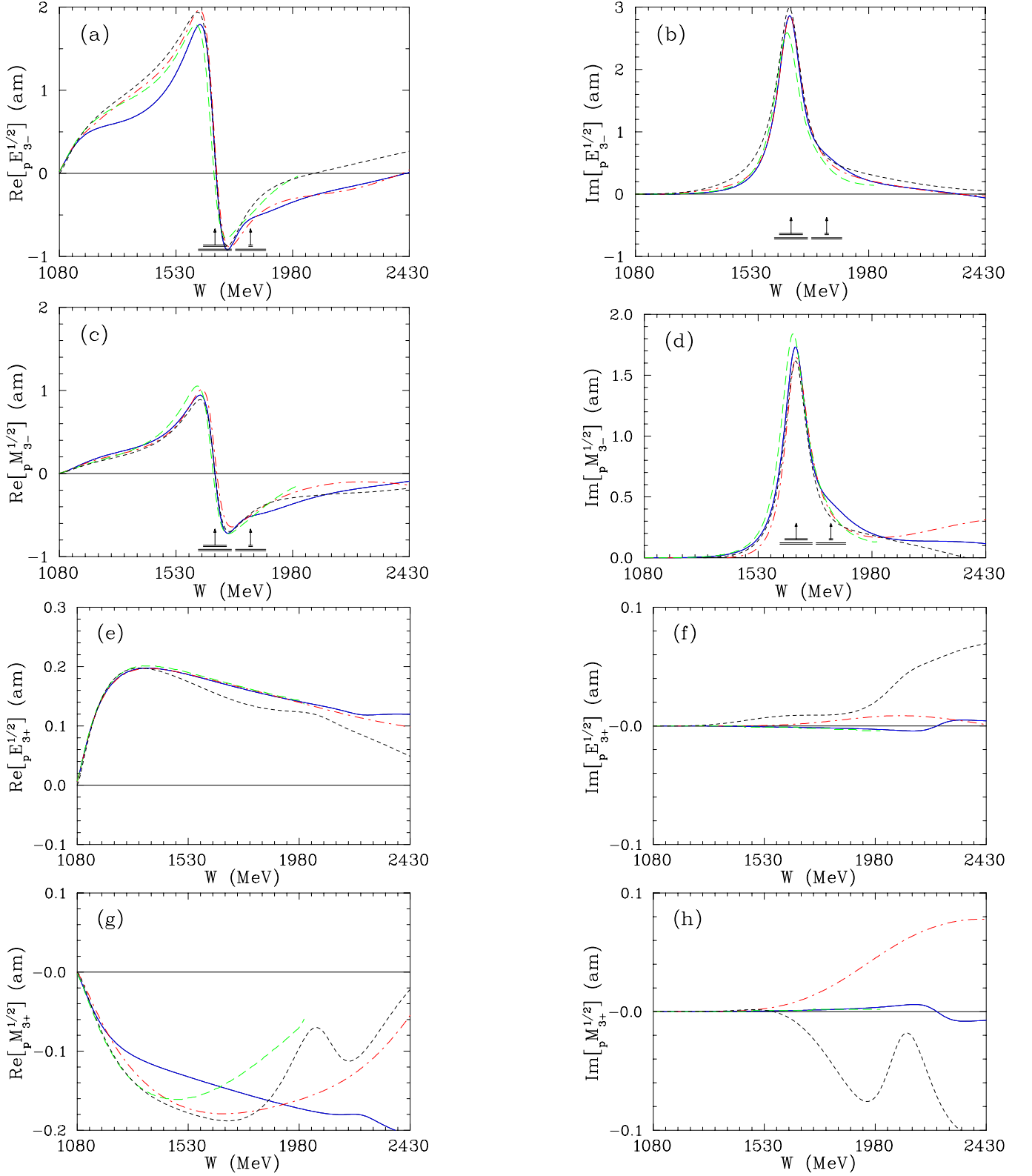


FIG. 6. (Color online) Notation of the multipoles is the same as in Fig. 4.

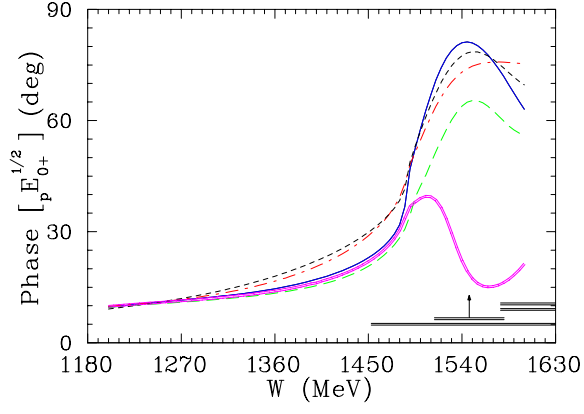


FIG. 7. (Color online) Phase for $pE_{0+}^{1/2}$ multipole. Notation of the solutions is the same as in Fig. 1. The thick solid line corresponds to the SAID πN solution SP06 [6] for the S_{11} phase shift.

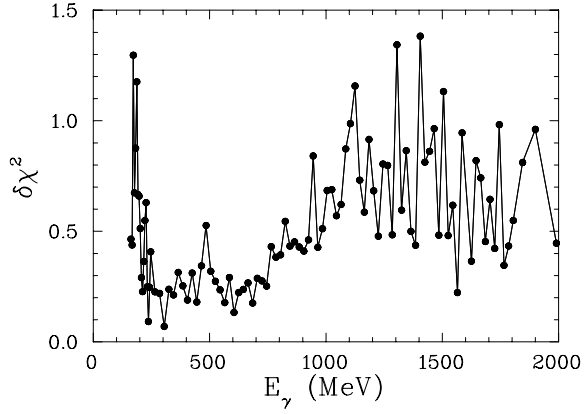


FIG. 8. Comparison of the SES and ED CM11 fits via $\delta\chi^2 = [\chi^2(\text{CM12}) - \chi^2(\text{SES})]/N_{\text{data}}$ versus laboratory photon energy E_γ .

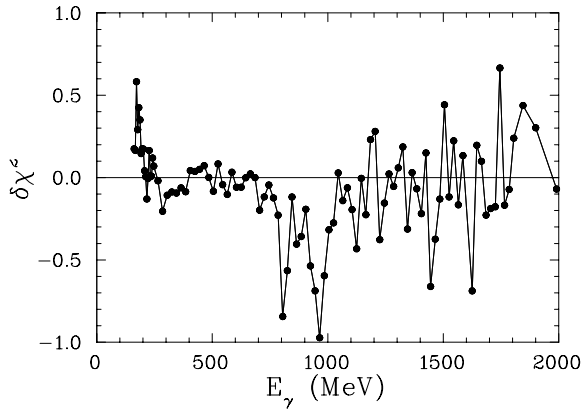


FIG. 9. Comparison of the CM12 and SN11 SES fits via $\delta\chi^2 = [\chi^2(\text{CM12}) - \chi^2(\text{SN11})]/N_{\text{data}}$ versus laboratory photon energy E_γ .